J. Fluid Mech. (1990), *vol.* 211, *pp.* 437–461
Printed in Great Britain

The three-dimensional stability of finite-amplitude convection in a layered porous medium heated from below

By D. A. S. REES† AND D. S. RILEY
School of Mathematics, University Walk, Bristol BS8 1TW, UK

(Received 30 November 1988 and in revised form 9 August 1989)

Landau–Ginzburg equations are derived and used to study the three-dimensional stability of convection in a layered porous medium of infinite horizontal extent. Criteria for the stability of convection with banded or square planform are determined and results are presented for two-layer and symmetric three-layer systems. In general the neutral curve is uni-modal and parameter space is divided into regions where either rolls or square cells are stable. For certain ranges of parameters, however, the neutral curve is bimodal and there exists a locus of parameters where two modes with different wavenumbers have simultaneous onset.

1. Introduction

Free convection in porous media has been the subject of considerable attention due to its importance in, for example, geothermal energy studies. Horton & Rogers (1945) and Lapwood (1948) were the first to show that, provided the Rayleigh number exceeds $4\pi^2$, convection cells can occur when a porous layer of infinite horizontal extent is uniformly heated from below. Experimental verification of this result was provided by Katto & Masuoka (1967). It was also confirmed by Westbrook (1969), using an energy stability method, and extended to finite domains by Beck (1972). Palm, Weber & Kvernvold (1972), using the method of Schlüter, Lortz & Busse (1965), showed that two-dimensional rolls constitute the stable pattern of convection near onset, but values for the range of stable wavenumbers were not presented. By using a spectral method, Straus (1974) determined the region of stability of rolls well into the strongly nonlinear regime, thus extending and verifying the work of Palm *et al.*

Subsequently, further realism has been sought by many authors. The separate effects of anisotropy and hydrodynamic dispersion on the stability of rolls were determined by Kvernvold & Tyvand (1979, 1980). The influence of aspect ratio on pattern selection was determined by, for example, Straus & Schubert (1981) and Riley & Winters (1989*a*), and on the onset of time-dependent motion by, for example, Caltagirone (1975) and Riley & Winters (1989*b*). Georgiadis & Catton (1986) considered the effects of a finite Darcy–Prandtl number, inertia and no-slip conditions on two-dimensional convection in an infinite layer. More recently Rees & Riley (1986, 1987, 1989 *a*, *b*) and Rees (1990) have considered the effects of small-amplitude imperfections at the horizontal boundaries. They show that, depending on the wavenumber and symmetry of the imperfections, various stable cellular patterns

† Present address: Mathematics Department, North Park Road, Exeter EX4 4QE, UK.

arise, including rolls, squares, rectangles and rolls with spatially varying phase or orientation. The effects of sidewall imperfections were studied by Impey, Riley & Winters (1990), who showed that the bifurcation structure is crucially dependent on the Fourier decomposition of the imperfection.

The above-mentioned studies have all been concerned with convection in homogeneous media; it is the purpose of this paper to address the problem of the onset and stability of convection in inhomogeneous layers, or, more specifically, in layered media. Georghitza (1961) was the first to consider the effects of inhomogeneities. Two problems were investigated: the first concerned a porous medium consisting of two sublayers with slightly different permeabilities; the second, a single layer with a permeability having a weak, linear dependence on the vertical coordinate. Donaldson (1962) used a finite-difference method to compute the flow and temperature field in a two-layer system, the lower layer of which was impermeable, but finitely conducting. Ribando & Torrance (1976) assumed an exponential variation in the ratio of viscosity to permeability. More recent works have concentrated directly on the effects of layering. Masuoka *et al.* (1978) derived criteria for the onset of convection in a two-layer system and also calculated flow patterns. Rana, Horne & Cheng (1979) used a three-layer system to model the Pahoa reservoir in Hawaii. A comprehensive analysis of the onset of convection and the post-critical heat transfer was presented by McKibbin & O'Sullivan (1980, 1981). This was extended to include the effects of thin, highly impermeable 'sheets' (McKibbin & Tyvand 1983) and thin highly permeable 'cracks' (McKibbin & Tyvand 1984) within the layer. McKibbin (1983) generalized Donaldson's work to include layers which do not have the same thickness or thermal conductivity.

In the above multilayer studies, and also in those involving other material inhomogeneities, the flow has been assumed to be two-dimensional. Owing to the presence of slip conditions in porous media flows, the results these papers describe are certainly valid for a medium which is narrow in the spanwise coordinate so that three-dimensional disturbances are suppressed. However, the question of the validity of the results in horizontally unbounded media is unresolved. We have partial information in that Riahi (1983) considered flow in a porous layer bounded above and below by semi-infinite regions of *impermeable*, conducting media and found that three-dimensional square cells constitute the stable planform in part of parameter space. It is the primary task of this paper to determine the preferred planform of convection near onset, thereby validating and extending the above results. Of major importance also are the stability boundaries, i.e. the range of stable wavenumbers, since these determine the possible variation in heat transfer.

Recent studies have concerned convection in related configurations. Catton & Lienhard (1984) and Heiber (1987) have analysed the onset of two-dimensional convection in multiple pure-fluid layers when the layers are separated by a rigid layer of finite conductivity and thickness. Lienhard & Catton (1986) extended these results by calculating the post-critical heat transfer coefficients. Criteria have also been derived for the onset of two-dimensional convection in coupled fluid/porous layers by Sommerton & Catton (1982) and Pillatsis, Taslim & Narusama (1987). Chen & Chen (1988) considered a model of double-diffusive convection in a porous layer underlying a fluid layer in order to describe channel segregation in the solidification of alloys. They performed a linear stability analysis showing that the neutral stability curve may be bimodal. Similar bimodality was found by Proctor & Jones (1988) who considered flow in a double Bénard layer, i.e. two layers of fluid separated by a rigid conducting membrane of zero thickness. They considered two-dimensional

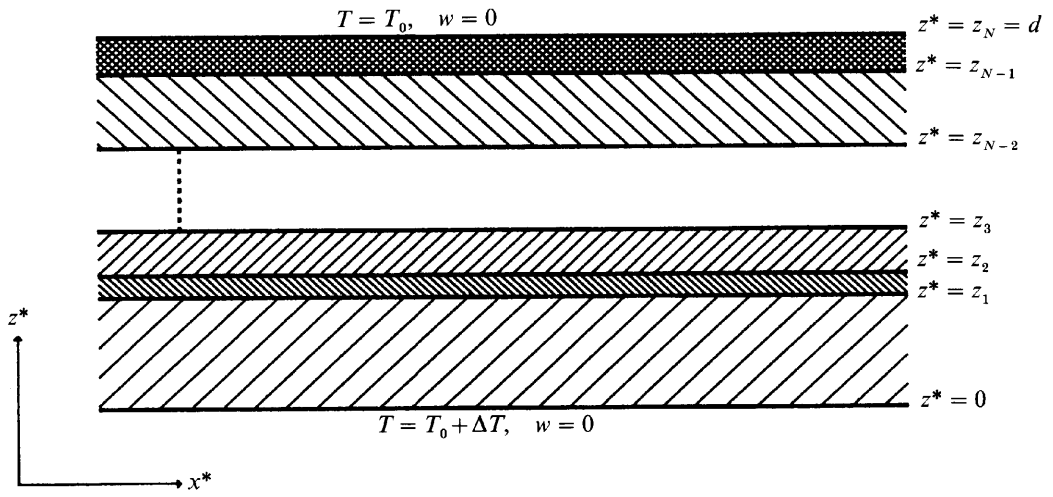

FIGURE 1. Definition sketch of the flow domain comprising a layered porous medium consisting of N homogeneous sublayers.

convection when two modes onset simultaneously with a wavenumber ratio of precisely 2 and found a rich bifurcation structure. Bimodality also arises in the present problem and is a consequence of layering.

The general layout of the paper is as follows. Section 2 contains a derivation of the governing equations and boundary and interface conditions for an arbitrary number of layers. A weakly nonlinear analysis is presented in §3 and it is shown that the amplitude of convection in the form of rolls (squares are the superposition of two orthogonal rolls) is governed by a set of coupled space-dependent Landau–Ginzburg equations similar in form to that for the Bénard problem. These equations are analysed in §4. Criteria for the stability of rolls and squares are given and bounds on the range of stable wavenumbers for both planforms are derived. In §§5 and 6 we present the main results of our analysis, the former containing results for two-layer systems, the latter for symmetric three-layer systems. In §7, our method is applied to the studies of Donaldson (1962) and Rana *et al.* (1979) confirming their assumption that the flow is two-dimensional. Finally, we discuss the results in §8.

2. Formulation of the problem

We consider a fluid-saturated porous layer which is heated uniformly from below and composed of N homogeneous sublayers (see figure 1). The outer horizontal boundaries, which are situated at $z^* = 0$ and $z^* = d$, are held at temperatures $T_0 + \Delta T$ and T_0, respectively, where $\Delta T > 0$, and are impermeable. The horizontal interfaces between the layers are assumed to be permeable. In each sublayer, conservation of mass, momentum and energy (suitably averaged over a representative elementary volume) determine the pressure P, relative to the pressure when the system is all at a temperature T_0; the Darcy velocity vector $\boldsymbol{q} = (u, v, w)$; and the temperature T:

$$\boldsymbol{\nabla} \cdot \boldsymbol{q} = 0, \tag{2.1}$$

$$\boldsymbol{q} = -\frac{K_i}{\mu}(\boldsymbol{\nabla} P + \rho\beta^*(T - T_0)\boldsymbol{g}), \tag{2.2}$$

$$[\phi_i \rho c + (1-\phi_i)\rho_i c_i]\frac{\partial T}{\partial t^*} + \rho c \boldsymbol{q} \cdot \boldsymbol{\nabla} T = k_i \boldsymbol{\nabla}^2 T. \tag{2.3}$$

Here the Darcy–Prandtl number has been assumed large so that inertia effects are negligible in (2.2), and the Boussinesq approximation has been invoked. In the above $\boldsymbol{g}$ is the gravity vector; ρ, c, μ and β^* are the density, specific heat, viscosity and coefficient of cubical expansion of the saturating fluid; ρ_i, c_i, K_i and ϕ_i are the density, specific heat, permeability and porosity of the ith sublayer matrix; k_i denotes the effective thermal conductivity of the ith saturated sublayer and t^* denotes time.

The outer boundary conditions are given by

$$T = T_0 + \Delta T, \quad w = 0 \quad \text{on } z^* = 0, \tag{2.4}$$

$$T = T_0, \quad w = 0 \quad \text{on } z^* = d. \tag{2.5}$$

At the interfaces between the sublayers, the temperature, pressure and vertical fluxes of mass and heat are taken to be continuous. We also assume that the net mass flux along the layer is zero.

To facilitate the analysis of the three-dimensional stability characteristics of finite-amplitude convection, we recast the above equations and boundary conditions in terms of the pressure and temperature fields. On eliminating $\boldsymbol{q}$ from (2.1)–(2.3) we obtain

$$\nabla^2 P = \rho_0 g\beta \frac{\partial T}{\partial z^*}, \tag{2.6}$$

$$\frac{k_i}{\rho c}\nabla^2 T = \frac{K_i}{\mu}\rho_0 g\beta^*(T - T_0)\frac{\partial T}{\partial z^*} - \frac{K_i}{\mu}\nabla P \cdot \nabla T + \lambda_i^* \frac{\partial T}{\partial t^*}, \tag{2.7}$$

where $\lambda_i^* = [\phi_i \rho c + (1-\phi_i)\rho_i c_i]/\rho c$. This system possesses a trivial 'conduction' solution with a piecewise-linear temperature distribution and no convection:

$$T_{ic} = T_0 + \Delta T\left[\frac{z_{i-1} - z^*}{k_i} + \sum_{j=1}^{N} \delta_j\right]\Big/\delta, \tag{2.8}$$

$$P_{ic} = \rho_0 g\beta^* \Delta T\left[-\frac{(z^* - z_{i-1})^2}{2k_i} + \sum_{j=1}^{N} \delta_j\left(z^* - \frac{z_j + z_{j-i}}{2}\right)\right]\Big/\delta. \tag{2.9}$$

In the above $\delta_i = d_i/k_i$, where d_i is the depth of the ith sublayer,

$$\delta = \sum_{j=1}^{N} \delta_j, \quad z_i = \sum_{j=1}^{i} d_j,$$

and $z_{i-1} < z^* < z_i$. The temperature drop across the ith sublayer is given by

$$\Delta T_i = \frac{\delta_i}{\delta}\Delta T. \tag{2.10}$$

It proves convenient to use a similar non-dimensionalization to that of McKibbin & O'Sullivan (1980, 1981). Therefore we set

$$(x^*, y^*) = d(x, y), \quad Z_i = \frac{z^* - z_{i-1}}{d_i}, \quad \theta_i = \frac{T - T_0}{\Delta T_i}, \quad p_i = \frac{K_i \rho c}{\mu r_i k_i} P, \quad t^* = \left(\frac{\rho c d^2}{k_n}\right) t \tag{2.11}$$

in (2.6) and (2.7), to obtain

$$r_i^2\left(\frac{\partial^2 p_i}{\partial x^2}+\frac{\partial^2 p_i}{\partial y^2}\right)+\frac{\partial^2 p_i}{\partial Z_i^2}-\frac{R_i}{r_i}\frac{\partial \theta_i}{\partial Z_i}=0, \tag{2.12}$$

$$r_i^2\left(\frac{\partial^2 \theta_i}{\partial x^2}+\frac{\partial^2 \theta_i}{\partial y^2}\right)+\frac{\partial^2 \theta_i}{\partial Z_i^2}=\left(R_i\theta_i-r_i\frac{\partial p_i}{\partial Z_i}\right)\frac{\partial \theta_i}{\partial Z_i}-r_i^3\left(\frac{\partial p_i}{\partial x}\frac{\partial \theta_i}{\partial x}+\frac{\partial p_i}{\partial y}\frac{\partial \theta_i}{\partial y}\right)+\lambda_i\frac{\partial \theta_i}{\partial t}, \tag{2.13}$$

where k_n is the thermal conductivity of a reference sublayer and $\lambda_i = \lambda_i^* r_i^2 k_n/k_i$. Here $r_i = d_i/d$ is the relative thickness of sublayer i compared with the depth of the whole layer, and R_i is a local Rayleigh number defined by

$$R_i = \frac{\rho_0 g\beta^* \Delta T_i d_i K_i \rho_i c_i}{\mu k_i}. \tag{2.14}$$

Thus in each sublayer the equations are non-dimensionalized differently and the corresponding z-coordinate, Z_i, takes values between 0 and 1.

The boundary conditions are now

$$\theta_1 = \frac{k_1}{r_1}\sum_{j=1}^{N}\frac{r_j}{k_j}, \quad k_1\frac{\partial p_1}{\partial z}-\frac{R_1 k_1}{r_1}\theta_1 = 0 \quad \text{on } Z_1 = 0, \tag{2.15}$$

$$\theta_N = 0, \quad \frac{\partial p_N}{\partial Z_N} = 0 \quad \text{on } Z_N = 1, \tag{2.16}$$

and the interface conditions at $Z_i = 1$ and $Z_{i+1} = 0$ are

$$\frac{r_i}{k_i}\theta_i = \frac{r_{i+1}}{k_{i+1}}\theta_{i+1}, \quad \frac{\partial \theta_i}{\partial Z_i} = \frac{\partial \theta_{i+1}}{\partial Z_{i+1}}, \quad \frac{k_i r_i}{K_i}p_i = \frac{k_{i+1} r_{i+1}}{K_{i+1}}p_{i+1}, \tag{2.17a–c}$$

$$k_i\frac{\partial p_i}{\partial Z_i}-\frac{R_i k_i}{r_i}\theta_i = k_{i+1}\frac{\partial p_{i+1}}{\partial Z_{i+1}}-\frac{R_{i+1}k_{i+1}}{r_{i+1}}\theta_{i+1}. \tag{2.17d}$$

For later reference we introduce R given by

$$R = \frac{\rho_0 g\beta^* \Delta T d K_n \rho c}{4\pi^2 \mu k_n}, \tag{2.18}$$

which is a global Rayleigh number given in terms of the total temperature drop and depth of the layer, the permeability and thermal conductivity of the reference sublayer, n, and is scaled relative to the critical Rayleigh number, $4\pi^2$, for a single layer. Using (2.14) and (2.18), a convenient alternative representation is given by

$$\frac{R_i}{R} = 4\pi^2 r_i^2\left(\frac{K_i k_n}{K_n k_i^2}\right)\Big/\sum_{j=1}^{N}\frac{r_j}{k_j}. \tag{2.19}$$

The heat transferred through the layer is a quantity of important practical interest. Therefore we introduce the Nusselt number, Nu, defined as the ratio of the heat transferred by convection and conduction to that transferred by conduction alone, and given by

$$Nu = -\frac{1}{L}\int_0^L \frac{\partial \theta_1}{\partial Z_1}\bigg|_{Z_1=0} \mathrm{d}x, \tag{2.20}$$

where we have assumed that convection takes the form of rolls with generators in the y-direction and wavelength L; for other modes of convection, such as square cells, the integration is over the appropriate region in (x, y)-space.

3. Weakly nonlinear expansion

The bifurcation to two-dimensional convection from the conduction solution was described by McKibbin & O'Sullivan (1980, 1981). Steady convection bifurcates supercritically at a critical Rayleigh number which is dependent on the particular configuration, and it is a straightforward, but lengthy, computation to find the post-critical Nusselt number. The assumption of two-dimensional flow is common to most previous investigations: Donaldson (1962), Masuoka *et al.* (1979), Rana *et al.* (1979), McKibbin (1983) and McKibbin & Tyvand (1983, 1984). Riahi (1983) showed, however, that when a single porous layer is bounded by finitely conducting, impermeable bedrock and caprock, three-dimensional flow with square planform can constitute a stable pattern. In view of this we shall consider general three-dimensional stability.

We use Newell–Whitehead–Segel theory and seek asymptotic expansions in powers of ϵ:

$$(p_i, \theta_i, R_i, R) = \sum_{n=0} \epsilon^n (p_i^{(n)}, \theta_i^{(n)}, R_i^{(n)}, R^{(n)}), \tag{3.1}$$

where $R^{(n)}$ and $R_i^{(n)}$ are related via (2.19) and $\epsilon \ll 1$ is the typical magnitude of the post-critical motion. Here $(p_i^{(0)}, \theta_i^{(0)})$ are given by

$$\frac{p_i^{(0)}}{R_i^{(0)}} = -\frac{Z_i^2}{2r_i} + \left(\frac{k_i}{r_i^2}\sum_{j=1}^{N}\frac{r_j}{k_j}\right)Z_i + \frac{k_i}{2r_i^3}\left(\sum_{j=i}^{N} r_j^2/k_j\right) + \frac{\mathrm{k_i}}{\mathrm{r_i^3}}\left(\sum_{j=1}^{i-1} r_j\right)\left(\sum_{j=i}^{N}\frac{r_j}{k_j}\right) - \frac{k_i}{r_i^3}\left(\sum_{j=i}^{N}\frac{r_j}{k_j}\sum_{l=1}^{j} r_l\right), \tag{3.2}$$

$$\theta_i^{(0)} = \frac{k_i}{r_i}\sum_{j=i}^{N}\frac{r_j}{k_j} - Z_i, \tag{3.3}$$

i.e. the non-dimensional conduction solution.

The solution to the $O(\epsilon)$-equations is taken to be the sum of two rolls of relative orientation ϕ:

$$\begin{pmatrix} p_i^{(1)} \\ \theta_i^{(1)} \end{pmatrix} = \tfrac{1}{2}(A\,\mathrm{e}^{\mathrm{i}\alpha x} + \bar{A}\,\mathrm{e}^{-\mathrm{i}\alpha x})\begin{pmatrix} f_i^{(0)} \\ g_i^{(0)} \end{pmatrix} + \tfrac{1}{2}(\mathrm{B}\,\mathrm{e}^{\mathrm{i}\alpha(x\cos\phi - y\sin\phi)} + \bar{B}\,\mathrm{e}^{-\mathrm{i}\alpha(x\cos\phi - y\sin\phi)})\begin{pmatrix} f_i^{(0)} \\ g_i^{(0)} \end{pmatrix}, \tag{3.4}$$

where the amplitudes, A and B, are functions of the slow timescale $\tau = \epsilon^2 t$ and, in the first instance, the slow spatial scales $X = \epsilon x$ and $Y = \epsilon y$. We note that the differential operators arising at $O(\epsilon)$ may be made self-adjoint by a suitable weighting of each equation *only* if the layer has a constant thermal conductivity – we assume this from now on. In general the application of the solvability condition, which is derived below, to the $O(\epsilon^2)$-equations yields the result that $R^{(1)} = 0$ (the exception occurs when second-order resonances arise – these are discussed later).

The solution to the $O(\epsilon^2)$-equations is complicated by the presence of terms involving the first-order partial derivatives of the amplitudes, but this does not prove too troublesome for they may be shown to be orthogonal to the eigenfunctions $(f_i^{(0)}, g_i^{(0)})$ and therefore are not involved in the solvability condition at second order. On proceeding to the solvability condition on the $O(\epsilon^3)$-equations we find terms involving the second spatial derivatives of the amplitudes. These terms, however,

simply reflect the curvature of the neutral curve near its minimum, and hence the required coefficient can be calculated from the linear stability problem. In this way we obtain

$$c_1 A_\tau = \sigma A + c_2 A_{XX} - c_3 A[A\bar{A} + c_4 B\bar{B}], \tag{3.5a}$$

$$c_1 B_\tau = \sigma B + c_2 B_{X_B X_B} - c_3 B[B\bar{B} + c_4 A\bar{A}], \tag{3.5b}$$

where $\sigma = R^{(2)}/R^{(0)}$, $X_B = X\cos\phi - Y\sin\phi$, and $c_2 \geqslant 0$ is the curvature-related coefficient. The values c_1, c_3 and c_4 are real functions of r_i and K_i ($i = 1(1)N$), and c_4 also depends on ϕ, the relative orientation of the rolls. It may be shown analytically that c_1 is positive and, numerically, we find that c_3 and c_4 are also positive.

In order to analyse the zigzag instability, we consider slightly oblique modes and define the slow spatial scales $X^* = \epsilon^{\frac{1}{2}}x$, $Y^* = \epsilon^{\frac{1}{2}}y$. Omitting all detail, we obtain

$$c_1 A_\tau = \sigma A + c_2\left[\frac{\partial}{\partial X} - \frac{\mathrm{i}}{2\alpha}\frac{\partial^2}{\partial Y^{*2}}\right]^2 A - c_3 A[A\bar{A} + c_4 B\bar{B}], \tag{3.6a}$$

$$c_1 B_\tau = \sigma B + c_2\left[\frac{\partial}{\partial X_B} - \frac{\mathrm{i}}{2\alpha}\frac{\partial^2}{\partial Y_B^{*2}}\right]^2 B - c_3 B[B\bar{B} + c_4 A\bar{A}], \tag{3.6b}$$

where $Y_B^* = Y^*\cos\phi + X^*\sin\phi$ and the coefficient of the $\partial^2/\partial Y^{*2}$ term in (3.6a) is chosen to be consistent with the behaviour of the neutral curve near its minimum. Thus when $A \propto \mathrm{e}^{\mathrm{i}(KX+LY^*)}$, the wavevector of the roll is $(\alpha+\epsilon K, \epsilon^{\frac{1}{2}}L)$ and its wavenumber is $\alpha+\epsilon(K+L^2/2\alpha)+o(\epsilon)$. When $K = -L^2/2\alpha$ the wavenumber becomes $\alpha+o(\epsilon)$. Likewise the effects of the space-dependent terms in (3.6a) cancel implying that, for a mode of wavenumber α, the critical value of σ is zero, as expected.

Convection in the form of any number of rolls may now be computed owing to the absence of further resonances in the weakly nonlinear expansion. For example if we consider convection in the form of three rolls of orientations 0, ϕ and χ and common wavenumber, α, then the respective amplitudes, A, B and C, of the rolls are given by

$$c_1 A_\tau = \sigma A - c_3 A[A\bar{A} + c_4(\phi) B\bar{B} + c_4(\chi) C\bar{C}], \tag{3.7a}$$

$$c_1 B_\tau = \sigma B - c_3 B[B\bar{B} + c_4(\phi) A\bar{A} + c_4(\chi-\phi) C\bar{C}], \tag{3.7b}$$

$$c_1 C_\tau = \sigma C - c_3 C[C\bar{C} + c_4(\chi-\phi) B\bar{B} + c_4(\chi) A\bar{A}], \tag{3.7c}$$

where the spatial derivatives have been omitted.

The heat transferred across the layer may now be computed: from (2.20) the Nusselt number is

$$Nu = 1 + \epsilon^2 Nu_2 (R^{(2)}/R^{(0)}), \tag{3.8a}$$

where

$$Nu_2 = \tfrac{1}{2}(A\bar{A} + B\bar{B} + C\bar{C})\left.\frac{\mathrm{d}g_1^{(0)}}{\mathrm{d}Z_1}\right|_{Z_1=0}. \tag{3.8b}$$

4. Analysis of the amplitude equations

The evolution of two rolls of finite relative orientation, ϕ, is governed by equations (3.5), where $c_4 = c_4(\phi) > 0$. When $\sigma > 0$ there is an infinity of possible steady solutions to these equations. They fall into two simple classes, namely pure modes for which one of A and B is zero, and mixed modes where both A and B are non-zero. The former class is typified by the roll solution

$$A = [(\sigma - c_2 K^2)/c_3]^{\frac{1}{2}}\mathrm{e}^{\mathrm{i}KX}, \quad B = 0, \tag{4.1}$$

where the solution has been normalized to be real at $X = 0$. The latter category is typified by the solution

$$A = A_0 e^{iKX}, \quad B = B_0 e^{iLX_B}, \tag{4.2}$$

where

$$|A_0|^2 = \frac{\sigma}{c_3(1+c_4)} + \frac{c_2(c_4 L^2 - K^2)}{c_3(1-c_4^2)}, \quad |B_0|^2 = \frac{\sigma}{c_3(1+c_4)} + \frac{c_2(c_4 K^2 - L^2)}{c_3(1-c_4^2)}. \tag{4.3a, b}$$

It is the stability of the solutions (4.1) and (4.2) with which we are concerned.

4.1. *The stability of roll solutions*

Consider first the stability of the pure mode given by (4.1). There are three forms of instability to which this steady solution may be subject, namely the zigzag, sideband and cross-roll instabilities. The analysis for the zigzag instability, using (3.6*a*), follows closely the analysis of Newell & Whitehead (1969) for the Bénard problem, and yields the result that modes with $K < 0$ are unstable to disturbances in the form of a pair of rolls equally oriented at an $O(\epsilon^{\frac{1}{2}})$-angle to the original roll. The disturbances subsequently evolve into a single roll. The sideband-instability result follows immediately from the analysis of Newell & Whitehead: the disturbance, which is of the form $e^{i(K+L)X} + c\, e^{i(K-L)X}$ where c is some constant, grows when

$$c_2 K^2 < \sigma < 3c_2 K^2, \tag{4.4}$$

where the lower bound represents the neutral curve for the A-mode.

The cross-roll instability is analysed by looking at B-mode disturbances using (3.5*b*). It is easily shown that the most unstable disturbance has the form $B =$ constant, i.e. it has precisely the critical wavenumber, and has that orientation ϕ which minimizes $c_4(\phi)$. In our numerical calculations this was generally achieved when $\phi = \frac{1}{2}\pi$; situations where this is not so are discussed in §5. Thus the disturbance is at right angles to the original mode and grows when

$$c_2 K^2 < \sigma < \frac{c_{4m}}{c_{4m}-1} c_2 K^2; \tag{4.5}$$

here $c_{4m} = \min_\phi c_4(\phi)$ is assumed to be greater than 1.

The relative importance of the sideband and cross-roll instabilities is gauged by comparing (4.4) and (4.5) whereupon we find that the cross-roll instability bound is a more restrictive bound on the wavenumber perturbation, K, when $c_{4m}/(c_{4m}-1) > 3$, that is, when

$$c_{4m} < \tfrac{3}{2}. \tag{4.6}$$

For a single porous layer $c_{4m} = 10/7 \approx 1.42857$ (Rees & Riley 1989*a*) and we recover the known result that the cross-roll instability is more important than the sideband instability.

Using (3.5) it is easily shown that rolls are unstable to cross-roll disturbances when

$$c_{4m} < 1, \tag{4.7}$$

whatever the value of K. As the fastest-growing disturbance is perpendicular to the original roll, the fully evolved flow pattern then has square planform and comprises two rolls as given by (4.2) and (4.3).

4.2. *The stability of square cells*

Having deduced the region of stability of rolls we now turn to the question of the stability of square cells. In order to simplify the analysis we assume that the constituent rolls have the same wavenumber and are given by

$$A = A_0 e^{iKX}, \quad B = A_0 e^{iKY}, \tag{4.8}$$

where $|A_0|^2 = (\sigma - c_2 K^2)/c_3(1+c_4)$, and $c_4 = c_4(\frac{1}{2}\pi)$. We consider four instability mechanisms corresponding to disturbances in the form of (i) the constituent rolls, (ii) sideband modes, (iii) zigzag modes and (iv) oblique rolls.

On introducing disturbances in the form of the constituent rolls it is simple to show that square cells are unstable whenever $c_4(\frac{1}{2}\pi) > 1$, which in view of (4.7) is not unexpected. Thus the planform of the stable mode of convection depends entirely on the value of c_4: when $c_4(\frac{1}{2}\pi) > 1$ rolls are stable and squares are unstable, and when $c_4(\frac{1}{2}\pi) < 1$ rolls are unstable and squares are stable. Moreover the same analysis also shows that rectangular cells comprising two rolls at relative orientation ϕ are stable whenever $c_4(\phi) < 1$.

The 'sideband' instability may be analysed by introducing the substitutions $A = A_0 e^{iKX} + \epsilon_A(X, Y)$, $B = A_0 e^{iKY} + \epsilon_B(X, Y)$ into (3.5), where $X_B = -Y$ as $\phi = \frac{1}{2}\pi$, and linearizing. The following equations are obtained for the disturbances ϵ_A and ϵ_B:

$$c_1 \frac{\partial \epsilon_A}{\partial \tau} = \sigma \epsilon_A + c_2 \frac{\partial^2 \epsilon_A}{\partial X^2} - c_3 |A_0|^2 [(2+c_4)\epsilon_A + e^{2iKX}\bar{\epsilon}_A + c_4 e^{iK(X+Y)}\bar{\epsilon}_B + c_4 e^{iK(X-Y)}\epsilon_B], \tag{4.9a}$$

$$c_1 \frac{\partial \epsilon_B}{\partial \tau} = \sigma \epsilon_B + c_2 \frac{\partial^2 \epsilon_B}{\partial Y^2} - c_3 |A_0|^2 [(2+c_4)\epsilon_B + e^{2iKY}\bar{\epsilon}_B + c_4 e^{iK(X+Y)}\bar{\epsilon}_A + c_4 e^{iK(Y-X)}\epsilon_A]. \tag{4.9b}$$

Solutions exist of the form

$$\epsilon_A = \epsilon_{A1} e^{i((K+L)X+MY)} + \epsilon_{A2} e^{i((K-L)X-MY)}, \tag{4.10a}$$

$$\epsilon_B = \epsilon_{B1} e^{i((K+M)Y+LX)} + \epsilon_{B2} e^{i((K-M)X-LY)}, \tag{4.10b}$$

where we note that the Y-variation in ϵ_A and the X-variation in ϵ_B give rise to $O(\epsilon^2)$ variations in the roll wavenumbers (and hence $O(\epsilon^4)$ variations in the Rayleigh number – a higher order than that which σ represents) and therefore both are passive variations in their respective equations, at least to the order of the present analysis. The resulting eigenvalue problem for the growth rates of ϵ_{A1}, ϵ_{A2}, ϵ_{B1} and ϵ_{B2} is found to decouple into two eigenvalue problems. One of these reproduces the result (4.4), the other yields the neutral curve

$$\sigma = c_2 K^2 \frac{(3+c_4)}{(1-c_4)}, \tag{4.11}$$

which is a more restrictive bound on stability than (4.4). Decoupling also occurs for the zigzag instability and yields the result as for rolls, namely that square cells with $K < 0$ are unstable.

Finally we look at disturbances in the form of rolls at an orientation ϕ_c relative to the A-roll. Using (3.7) and (4.2), the linearized equation governing the corresponding amplitude, C, is given by

$$c_1 C_\tau = [\sigma - c_3(c_4(\phi_c) + c_4(\tfrac{1}{2}\pi - \phi_c))|A_0|^2] C. \tag{4.12}$$

This may be rewritten in the form

$$c_1 C_r = [[\chi(\phi_c)\sigma + c_2 K^2(c_4(\phi_c) + c_4(\tfrac{1}{2}\pi - \phi_c))]/(1 + c_4(\tfrac{1}{2}\pi))]\, C, \tag{4.13}$$

where $\chi(\phi_c) = 1 + c_4(\frac{1}{2}\pi) - c_4(\phi_c) - c_4(\frac{1}{2}\pi - \phi_c)$, and the disturbance has precisely the critical wavenumber which maximizes the growth rate. We know that $(\mathrm{d}/\mathrm{d}\phi)$ $c_4(\phi) = 0$ at both $\phi_c = 0$ and $\phi_c = \frac{1}{2}\pi$ because $c_4(\xi) = c_4(-\xi) = c_4(\pi - \xi)$, and therefore it can be shown that $\chi(\phi_c)$ has turning values at $\phi_c = 0$, $\frac{1}{4}\pi$ and $\frac{1}{2}\pi$. The substitution of the first and third of these values into (4.13) yields the marginal curve above which disturbances grow:

$$\sigma = c_2 K^2(2 + c_4(\tfrac{1}{2}\pi)), \tag{4.14}$$

since $c_4(0) = 2$. This stability bound, however, is less restrictive than that for the sideband instability, (4.4), as $c_4(\frac{1}{2}\pi) < 1$. On substituting $\phi_c = \frac{1}{4}\pi$ into (4.13) we obtain the marginal curve

$$\sigma = \frac{2c_2\, c_4(\frac{1}{4}\pi)\, K^2}{2c_4(\frac{1}{4}\pi) - 1 - c_4(\frac{1}{2}\pi)}. \tag{4.15}$$

In all our calculations the denominator of (4.15) was found to be positive, implying that square cells are stable to C-mode disturbances above this curve. If the denominator were negative, then a similar analysis shows that square cells are unstable to C-mode disturbances with $\phi_c = \frac{1}{4}\pi$.

It is now a simple matter to determine the relative importance of this oblique roll instability mechanism and the sideband instability. On defining Γ such that

$$\Gamma = \frac{[3 + c_4(\frac{1}{2}\pi)][2c_4(\frac{1}{4}\pi) - 1 - c_4(\frac{1}{2}\pi)]}{2[1 - c_4(\frac{1}{2}\pi)]\, c_4(\frac{1}{2}\pi)} \tag{4.16}$$

then $\Gamma > 1$ implies that the sideband instability dominates, and vice versa. We find numerically that $\Gamma \gtrsim 30$ and therefore the sideband instability dominates the oblique roll instability.

5. Numerical results for the two-layer configuration

We first present our results for a porous layer consisting of two sublayers. As stressed by McKibbin & O'Sullivan (1980, 1981) there is a wide variety of configurations to consider even for a two-layer system. In the case of equal thermal properties in each sublayer it is possible, however, to present an exhaustive survey of the situation at the onset of convection. We have assumed the layers to be of infinite horizontal extent with the lower sublayer (sublayer 1) as the reference layer and therefore the results are functions of the two parameters, r_1 and K_2/K_1.

Values of the (global) critical Rayleigh number and wavenumber for this configuration were presented in McKibbin & O'Sullivan (1980) as a function of K_2/K_1 for $10r_1 = 1(1)9$. They found, in common with Masuoka *et al.* (1979), that for certain values of the parameters two minima exist on the critical-Rayleigh-number curve. However, this was mentioned only briefly and no cases were presented where the critical curve had two minima at the same value of the Rayleigh number. Contours of the critical Rayleigh number are shown in figure 2 for values of r_1 and K_2/K_1 lying between 0.01 and 1.0. We note that the results obtained by inverting the sublayers, i.e. interchanging (r_1, K_1) and (r_2, K_2) are identical to those presented here. It may be seen that, when either $K_2/K_1 = 1$ or $r_1 = 1, R_c = 1$, which is the appropriate scaled

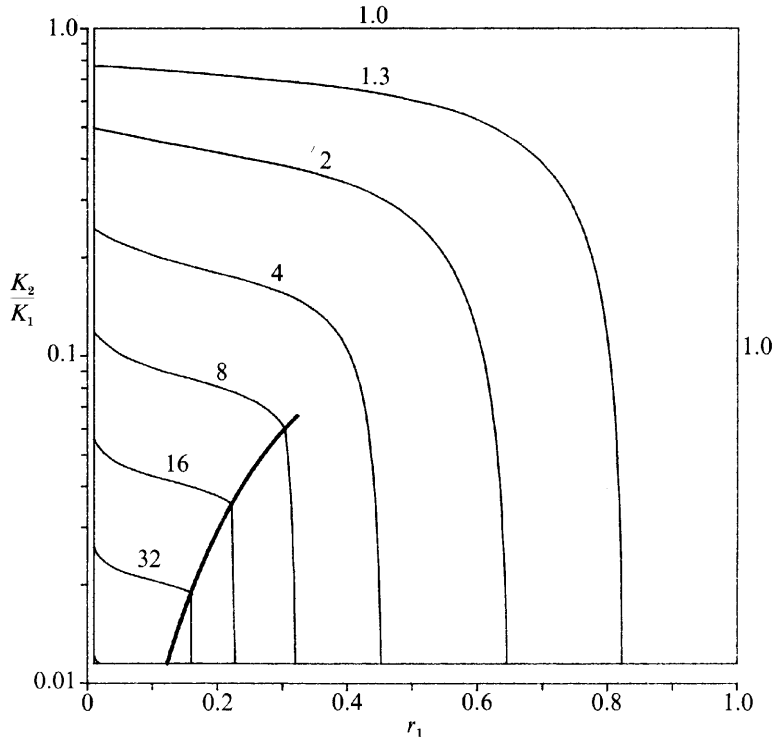

FIGURE 2. Values of the critical Rayleigh number, $R^{(0)}$, as a function of r_1 and K_2/K_1 for the two-layer system. The thick line denotes the double-minimum locus; this convention also applies for all other contour plots presented here.

value for the Lapwood (or single-layer) problem. Moreover the critical Rayleigh number, having been scaled with respect to the properties of sublayer 1, takes the value K_1/K_2 when $r_1 = 0$. The heavy line in figure 2 traces the double-minimum locus, the presence of which is also indicated by a discontinuity in the slope of the contours. This locus also represents the points at which the critical wavenumber for the onset of convection changes discontinuously. Values of α_c/π (π is the critical wavenumber for the Lapwood problem) are shown in figure 3 where this discontinuity is clearly evident. When $r_1 = 0$, $r_1 = 1$ or $K_2/K_1 = 1$ then $\alpha_c/\pi = 1$ as the configuration is equivalent to a single layer. For small values of K_2/K_1 the critical wavenumber becomes larger as r_1 decreases and the convection pattern becomes increasingly concentrated within the more permeable sublayer (see figure 3*b* in McKibbin & O'Sullivan 1980 for a typical example). As r_1 decreases further and $(r_1, K_2/K_1)$ crosses the double-minimum locus the most unstable mode suddenly switches to one with a global convection pattern (i.e. most of the fluid circulates through both sublayers; see figure 3*a* in McKibbin & O'Sullivan 1980), and with α_c/π taking a value nearer to 1.

One very interesting feature of these results not previously noted occurs at the end of the double-minimum locus. As the locus is traversed upwards, as drawn, the two critical wavenumbers approach each other and coincide at the end point. Thus the critical-Rayleigh-number curve has a single minimum there, but it is a quartic rather than a quadratic turning point. This is seen in figure 4 where we show successive critical curves corresponding to points on the double-minimum locus together with the locus of their minimum values. The quartic point corresponds to the values $r_1 = 0.323889$, $K_2/K_1 = 0.0657659$, $R_c = 6.917323$ and $\alpha_c/\pi = 1.540927$. These values were obtained using the classical fourth-order Runge-Kutta method with a constant

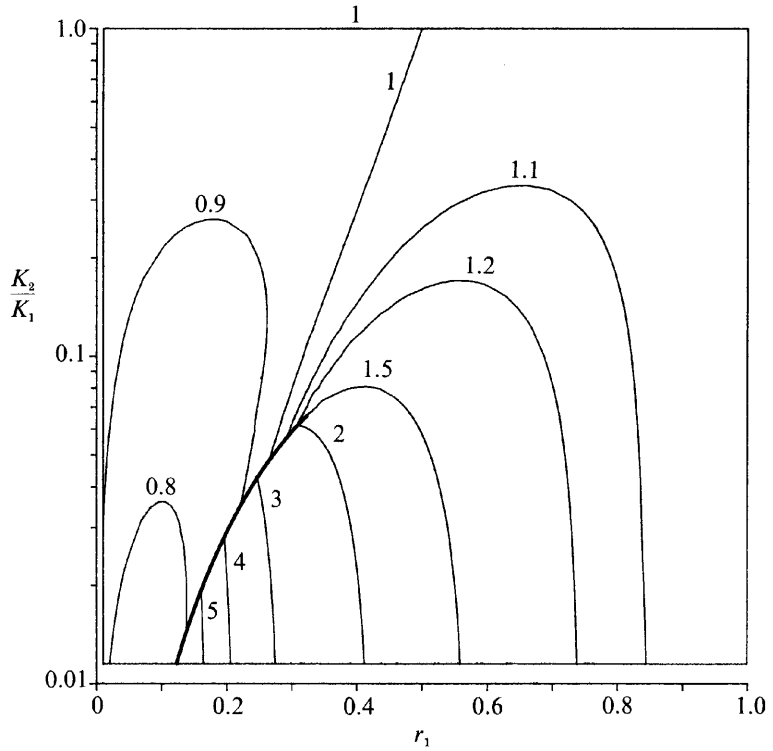

FIGURE 3. Values of the scaled wavenumber, α_c/π, as a function of r_1 and K_2/K_1 for the two-layer system.

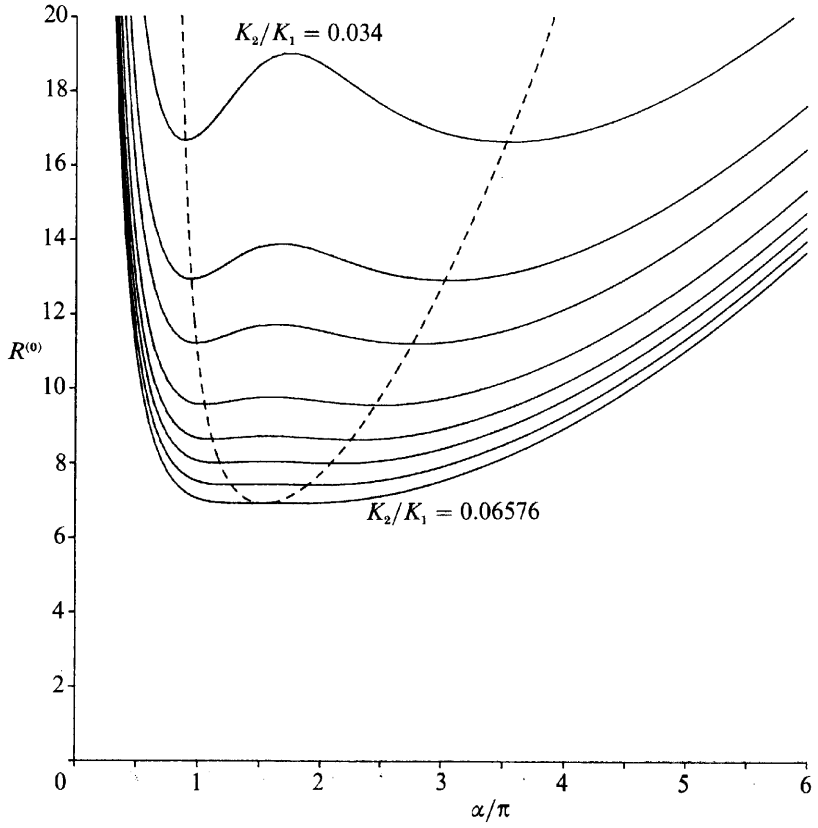

FIGURE 4. Neutral curves corresponding to values of $(r_1, K_2/K_1)$ lying on the double-minimum locus for the two-layer system. The curves correspond to $K_2/K_1 = 0.06576$, 0.063, 0.06, 0.057, 0.053, 0.047, 0.042, 0.034. The dashed line denotes the locus of the respective minima.

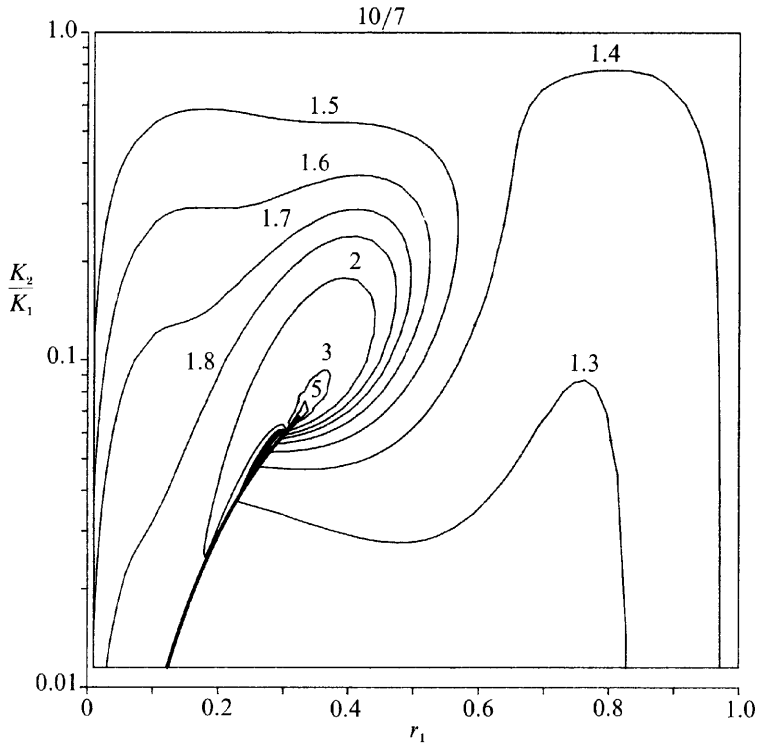

FIGURE 5. Values of the coupling parameter, $c_4(\frac{1}{2}\pi)$, as a function of r_1 and K_2/K_1 for the two-layer system. Values of c_4 above 1.5 correspond to regions where the sideband instability restricts the range of stable wavenumbers of rolls more than the cross-roll instability, and vice versa.

step-length to solve for $f_i^{(0)}$ and $g_i^{(0)}$ together with their first three derivatives with respect to α, and by setting $R_\alpha = R_{\alpha\alpha} = R_{\alpha\alpha\alpha} = 0$. Additional accuracy was obtained using Richardson extrapolation.

In figure 5 we show values of $c_4(\frac{1}{2}\pi)$ as a function of r_1 and K_2/K_1. There is a large region of parameter space where $c_4 > \frac{3}{2}$ which is the condition for the sideband instability to be more important than the cross-roll instability. Near the quartic point the values of $c_4(\frac{1}{2}\pi)$ increase rapidly, which therefore seems to herald a singularity. A careful study of the corresponding numerical values indicates that the singularity occurs at $r_1 = 0.316484$, $K_2/K_1 = 0.0636392$ for the smaller of the two wavenumbers on the double-minimum locus. Here the ratio of the critical wavenumbers is $\sqrt{2}$, and the singularity in $c_4(\frac{1}{2}\pi)$ is caused by the blow-up of the second-order solutions. On defining the critical wavenumbers to be α_1 and α_2, where $\alpha_1 < \alpha_2$, the second-order interaction of two modes with wavevectors $(\alpha_1, 0)$ and $(0, \alpha_1)$ gives rise to forcing terms with wavevectors $(\alpha_1, -\alpha_1)$ and (α_1, α_1), and therefore both have wavenumber $\sqrt{2}\alpha_1$. In general, when $\alpha_2 = \sqrt{2}\alpha_1$, the forcing terms contain components proportional to modes with orientation $\pm\frac{1}{4}\pi$ and wavenumber α_2. In a similar manner two modes with the higher wavenumber may interact at second order to generate a forcing term proportional to a mode with the lower wavenumber providing that their relative orientation has the appropriate value. This type of resonance occurs at all points on the double-minimum locus and therefore invalidates our analysis there. It is also worth noting that the values of both Nu_2 and $c_4(\frac{1}{4}\pi)$ for the smaller wavenumber tend towards zero as $\alpha_2/\alpha_1 \to 2$, owing to a second-order resonance. This in turn implies that $c_3 \to \infty$ since Nu_2 is inversely proportional to c_3. The coefficient $c_3 c_4$ remains bounded, however, since the solutions involved in its determination remain bounded and so $c_4 \to 0$ also. Codimension-two problems with

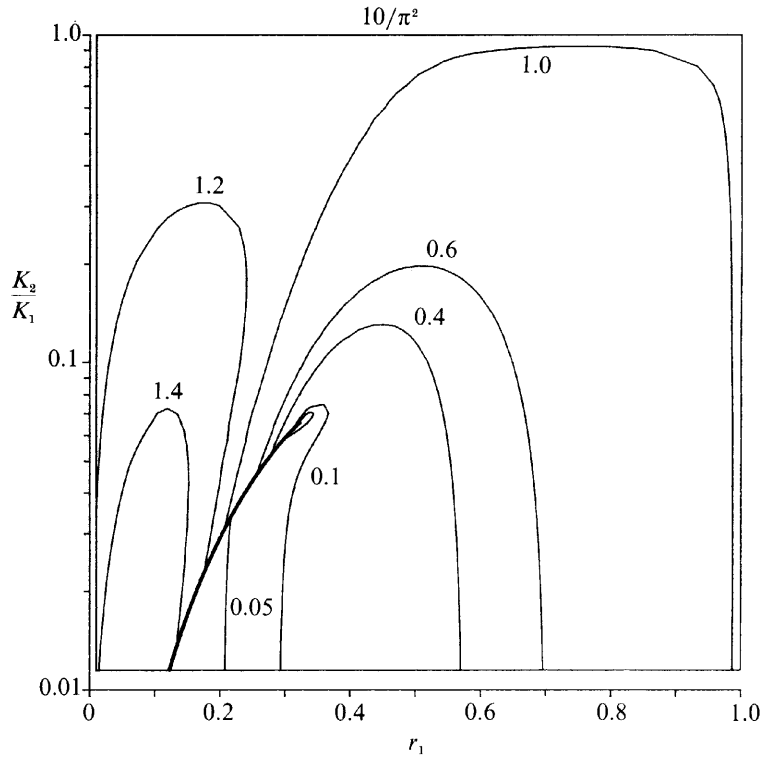

FIGURE 6. Values of the scaled curvature term, $10c_2$, as a function of r_1 and K_2/K_1 for the two-layer system.

$O(2)$ symmetry in which two modes with wavenumbers in the ratio 1:2 have simultaneous onset are of general interest. Studies by Armbruster, Guckenheimer & Holmes (1988), Jones & Proctor (1987) and Proctor & Jones (1988) have revealed a rich dynamical structure including heteroclinic cycles and modulated travelling waves. This aspect, however, lies outside the scope of the present work.

Thus, for parameter values on the double-minimum locus, the general analysis detailed in §§3 and 4, breaks down owing to resonant effects between the two wavelengths. At such points amplitude equations arise with only quadratic nonlinearities, implying the existence of transcritical bifurcations and flow at Rayleigh numbers below the critical value for linear instability. We note that when this is the case the effect of small perturbations in r_1 and K_2/K_1 will do little to affect this qualitative behaviour, and therefore doubt must be cast on the validity of our results in the region near to the double-minimum locus. The determination of the degree of subcriticality of convection and the region of validity of our results requires a fully nonlinear numerical computation.

Finally, in figure 6 we present values of c_2, which primarily determines the size of the band of wavenumbers that are linearly unstable when the Rayleigh number is just supercritical. When c_2 is relatively large this band is narrower than when c_2 is small (cf. Riley & Davis 1989). Values of c_2 on the left side of the locus are larger than the corresponding values on the right side, so that there is a larger range of unstable wavenumbers on the left side (see figure 4); the left side also corresponds to smaller wavenumbers (see figure 3). As the quartic point is approached c_2 decreases to zero, as expected. The values of c_2, in conjunction with the values of $c_4(\frac{1}{2}\pi)$ shown in figure 5, also determine the region of stability of rolls in Rayleigh number–wavenumber space. Whenever $c_4 > \frac{3}{2}$ the stability region is bounded by $\sigma = 3c_2K^2$, otherwise the bound is given by (4.5).

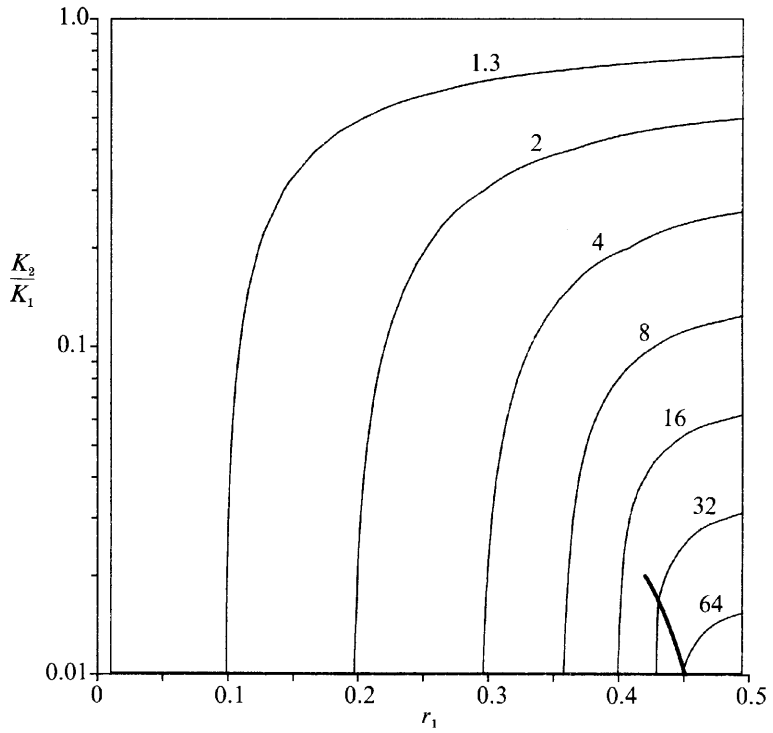

FIGURE 7. Values of the critical Rayleigh number $R^{(0)}$, as a function of r_1 and K_1/K_2 for the three-layer system (*a*).

As regards the heat transfer through the layer, we find it is greater when the convection pattern is global (relatively small α) than when convection is localized in one sublayer.

6. Numerical results for symmetric three-layer configurations

In this section we present the numerical results for symmetric configurations consisting of three sublayers, for which $k_1 = k_2 = k_3$, $r_1 = r_3$ and $K_1 = K_3$. We expect that the results for *non-symmetric* layers are qualitatively the same as those presented for the two-layer configuration as regards the existence of double-minimum points and the presence of second-order resonant terms.

Again, there are only two free parameters, r_1 and K_1/K_2, so that the whole of parameter space may be explored. We subdivide the presentation of the results into two parts: (*a*) those configurations for which the middle sublayer is more permeable than the outer sublayers, and (*b*) those for which it is less permeable. For (*a*) the middle layer was taken as the reference sublayer and the parameters r_1 and K_1/K_2 ($\leqslant 1$) varied. For (*b*) the lowest sublayer (sublayer 1) was taken as the reference sublayer and r_1 and K_2/K_1 ($\leqslant 1$) varied.

(*a*) Values of the critical (global) Rayleigh number for the specific case $r_1 = r_3 = 0.4$, $r_2 = 0.2$, $\alpha = \pi$ (rolls of square cross-section) are given in McKibbin & O'Sullivan (1980) for various values of K_2/K_1. By restricting themselves to one chosen wavenumber and one set of sublayer thicknesses they did not discover the presence of double-minimum points for this configuration. The locus of double-minimum points is shown as a heavy line on the critical-Rayleigh-number plot depicted in figure 7. Again the critical Rayleigh number increases as the thickness of the less

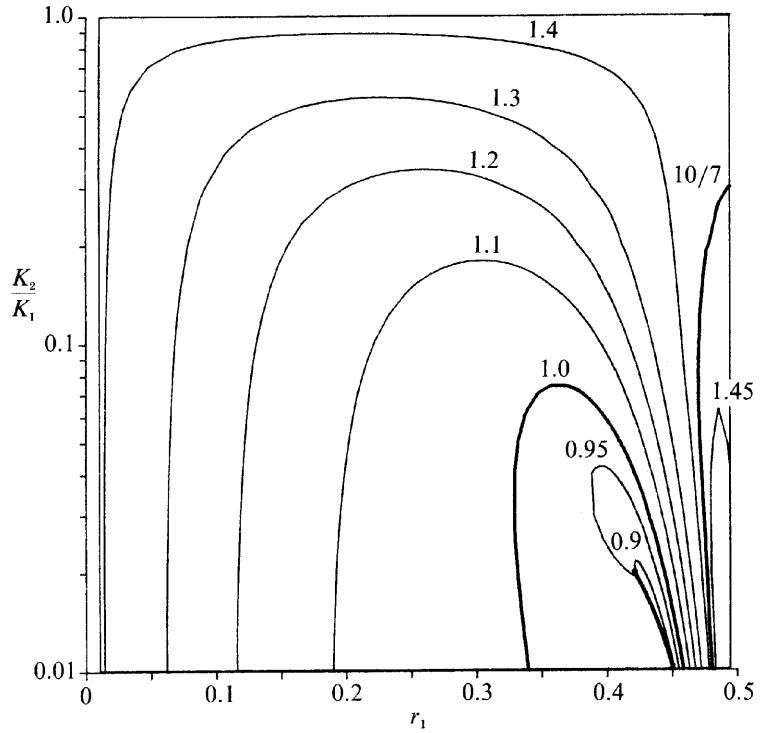

FIGURE 8. Values of the coupling parameter, $c_4(\frac{1}{2}\pi)$, as a function of r_1 and K_1/K_2 for the three-layer system (*a*). The second thick line denoting $c_4(\frac{1}{2}\pi) = 1$ divides parameter space into two regions where either rolls ($c_4 > 1$) or square cells ($c_4 < 1$) are stable. The single-layer value is given by $c_4(\frac{1}{2}\pi) = 10/7$.

permeable sublayer increases. The critical-wavenumber values just to the right of the double-minimum locus do not deviate greatly from π and correspond to a global flow pattern, as defined in the previous section. This occurs because the thin, but highly permeable, middle sublayer has little effect on the flow pattern; such behaviour was noted by McKibbin & Tyvand (1984) who studied the effect of 'cracks', or thin, highly permeable sublayers, on the onset of two-dimensional convection and the subsequent heat transfer. The corresponding critical Rayleigh numbers have values near to K_2/K_1 since the Rayleigh number is defined relative to sublayer 2. Just to the left of the double-minimum locus, however, the critical wavenumber is large compared with π and the flow is localized within the central sublayer. The end-point of the locus again corresponds to a quartic turning point, which arises at $r_1 = 0.419940$, $K_1/K_2 = 0.0202078$ with $R_c = 23.26715$ and $\alpha_c/\pi = 2.301403$.

Values of $c_4(\frac{1}{2}\pi)$ are shown in figure 8: there is a region where $c_4(\frac{1}{2}\pi) < 1$ within which rolls are unstable and square cells constitute a (linearly) stable mode of convection. It is interesting to note that the region contains the double-minimum locus itself and this could therefore have important ramifications on pattern selection as the locus is crossed. We note also that the values of $c_4(\frac{1}{2}\pi)$ are bounded above by 2, indicating that there are no singular solutions at second order, as is the case for two-layer configurations. Indeed this assertion may be proved by considering the up–down symmetry of the Z_i-dependent parts of the $O(\epsilon)$- and $O(\epsilon^2)$-terms (see also Jones & Proctor 1988). The first-order solutions are even about the midlayer plane and can only generate odd forcing terms at second order. Since the eigensolutions are even these forcing terms do not cause a resonance even if the wavenumber takes the critical value. We conclude, therefore, that our analysis is generally valid as no

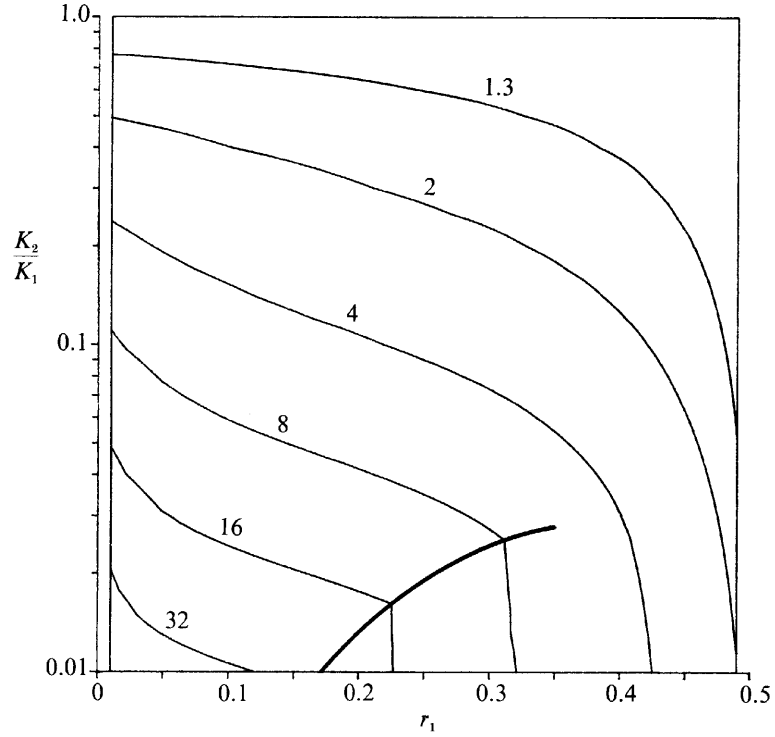

FIGURE 9. Values of the critical Rayleigh number, $R^{(0)}$, as a function of r_1 and K_2/K_1 for the three-layer system (*b*).

singularities arise at second order. Similarly this conclusion is valid for *all* symmetric configurations; the $O(\epsilon^2)$-singularities occurring on the double-minimum locus will arise for all non-symmetric configurations provided that they do indeed possess a double-minimum locus.

We do need to be aware, however, that other resonances may arise for symmetric configurations at third order, for example when the critical wavenumbers are α_1 and $\alpha_2 = 3\alpha_1$. We hope to study these higher-order resonances in the future, but, in the meantime, it is important to note that the effect of these resonances may be shown to apply only within $O(\epsilon^2)$ of the double-minimum locus. Thus the present analysis is valid but needs modification very close to the double-minimum locus.

As in the case of the two-sublayer configuration, we find that the larger heat transfer values occur when the circulation is global.

(*b*) We turn now to the complementary case where the middle sublayer is less permeable than the outer layers. Values of the critical Rayleigh number are shown in figure 9; again we note the presence of a double-minimum locus. In this configuration we have convection consisting of corotating vertical cells localized within the outer layers for parameter cases to the right of the double-minimum locus (see figure 8*a* in McKibbin & O'Sullivan 1980). Here there is relatively little flow within the middle sublayer. For parameter values lying just to the left of the locus, the flow is global in character but has a relatively small wavenumber. As the outer sublayers become thinner and more permeable, the inner boundaries begin to imitate constant-pressure surfaces. The flow then consists of nearly vertical flow through the middle sublayer with almost all the fluid being discharged into or entrained from the outer sublayers (see figure 8*c* in McKibbin & O'Sullivan 1980). The critical

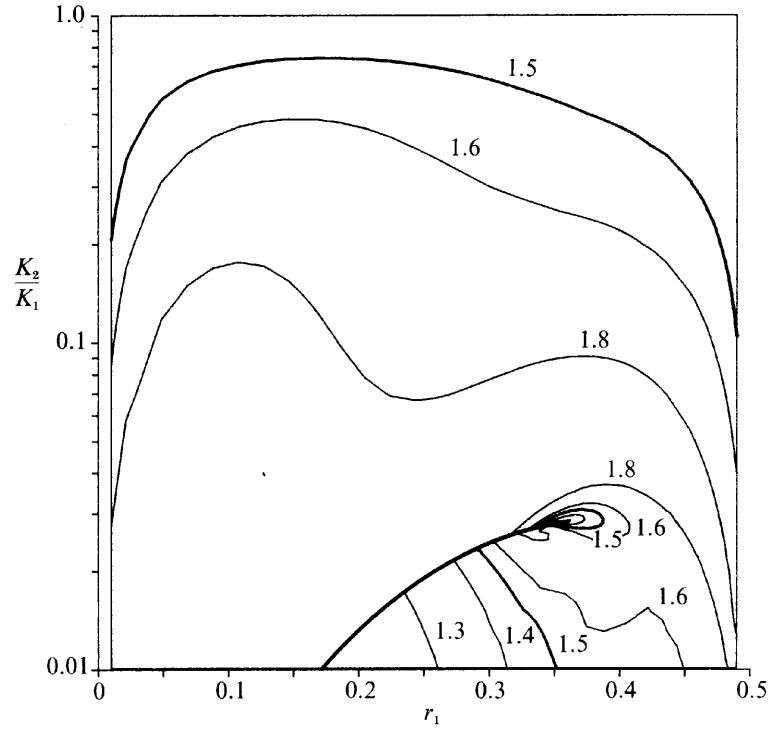

FIGURE 10. Values of the coupling parameter, $c_4(\frac{1}{2}\pi)$, as a function of r_1 and K_2/K_1 for the three-layer system (*b*). Values of c_4 above 1.5 correspond to regions where the sideband instability restricts the range of stable wavenumbers of rolls more than the cross-roll instability, and vice versa.

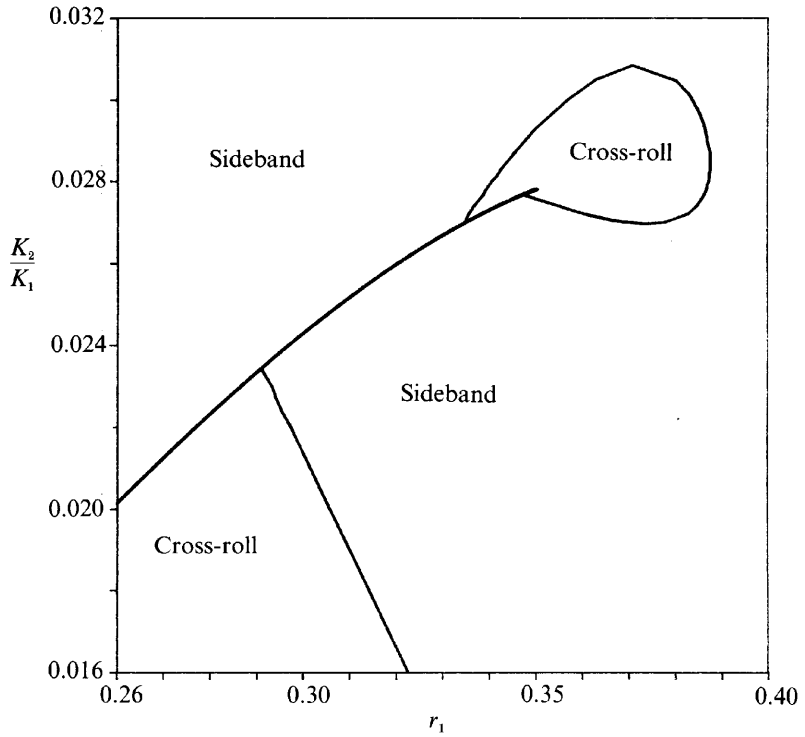

FIGURE 11. A close-up view of the $c_4(\frac{1}{2}\pi) = 1.5$ contour near the quartic point for the three-layer system (*b*).

wavenumber for a single layer with constant-pressure boundaries may be shown to be zero; values lying to the left of the double-minimum locus are decreasing as K_2/K_1 decreases.

Yet again there is a quartic turning point, which is located at $r_1 = 0.350339$, $K_2/K_1 = 0.0278195$ where $R_c = 5.966713$ and $\alpha_c = 1.195315\pi$.

Values of $c_4(\frac{1}{2}\pi)$ for case (*b*) are presented in figure 10. We see that, in most of the parameter space, $c_4(\frac{1}{2}\pi) > \frac{3}{2}$, which means that the sideband instability is more important than the cross-roll instability. The boundary where the sideband and cross-roll instabilities have equal importance and which is given by $c_4(\frac{1}{2}\pi) = \frac{3}{2}$ now assumes a rather complicated form. To clarify the situation, the part of the boundary near the quartic point is rescaled and shown in figure 11. Again $c_4(\frac{1}{2}\pi)$ is bounded for reasons of symmetry, as in (*a*). Once more third-order resonances arise which complicate the analysis within $O(\epsilon^2)$ of the double-minimum locus in parameter space. However, the resulting analysis is likely to be simpler than in (*a*) since rolls, rather than squares, are the stable planform on both sides of the double-minimum locus. Yet again we find relatively high heat transfer values when the wavenumber is small and the flow is global.

7. Application of the method to previous studies

There are, to our knowledge, only two studies other than those of McKibbin and his coworkers to which we can apply our method. The earlier of these studies consists of a numerical analysis (using finite differences) of the flow in a porous layer overlying an impermeable layer of equal thickness and thermal conductivity (Donaldson 1962). The flow was assumed to be two-dimensional and the upper boundary was either impermeable (closed-top), or at a constant pressure in order to simulate an open-top reservoir. This latter condition is very easily accommodated into our numerical scheme.

The configuration studied by Donaldson corresponds to our parameters $r_1 = r_2 = \frac{1}{2}$, $k_1/k_2 = 1$ and $K_1/K_2 = 0$, and to taking sublayer 2, the upper sublayer, as the reference sublayer. Although our numerical method does not apply when $K_1/K_2 = 0$, we found that setting K_1/K_2 as small as 10^{-5} does give reasonably accurate results. In tables 1 and 2 we present numerical results for this two-layer configuration for values of the permeability ratio varying from 1 to 10^{-5}, where the upper boundary is assumed to be either impermeable or at constant pressure. Values of R_c, α_c, Nu_2, $c_4(\frac{1}{2}\pi)$, $c_4(\frac{1}{3}\pi)$, $c_4(\frac{1}{4}\pi)$, $c_4(\frac{1}{6}\pi)$ and c_2 are given and are seen to converge as K_1/K_2 becomes small. For the closed-top case (table 1) there is a small range of the permeability ratio for which the sideband instability is more important than the cross-roll instability (i.e. when $c_4(\frac{1}{2}\pi) > 1.5$). For very small values of K_1/K_2, $c_4(\frac{1}{2}\pi) = 1.2495$, which yields the following expressions for the neutral, sideband instability and cross-roll instability curves:

$$\sigma = c_2 K^2, \quad \sigma = 3c_2 K^2, \quad \sigma = 5.0080 c_2 K^2, \tag{7.1}$$

respectively. Hence the region of stability of rolls is quite small compared with the region of existence of rolls. The limiting values of R_c and α_c are 3.3455 and 1.6954, respectively, which are in accord with McKibbin (1983). The corresponding results for the open-top case are given in table 2, where it may be seen that, since $c_4(\frac{1}{2}\pi) > \frac{3}{2}$ for all values of K_1/K_2, the sideband instability is more important than the cross-roll instability. Thus we have confirmed that two-dimensional rolls constitute the

K_1/K_2	R_c	α_c/π	Nu_2	$c_4(\frac{1}{2}\pi)$	$c_4(\frac{1}{3}\pi)$	$c_4(\frac{1}{4}\pi)$	$c_4(\frac{1}{6}\pi)$	$10c_2$
0.00001	3.3455	1.6954	0.5242	1.2495	1.4061	1.5767	1.7691	0.2983
0.00003	3.3454	1.6953	0.5242	1.2496	1.4062	1.5768	1.7691	0.2983
0.0001	3.3451	1.6951	0.5242	1.2497	1.4063	1.5769	1.7693	0.2984
0.0003	3.3441	1.6945	0.5245	1.2500	1.4066	1.5774	1.7698	0.2984
0.001	3.3408	1.6924	0.5252	1.2510	1.4080	1.5790	1.7714	0.2985
0.003	3.3311	1.6863	0.5272	1.2539	1.4118	1.5836	1.7762	0.2988
0.01	3.2969	1.6646	0.5350	1.2651	1.4260	1.6007	1.7932	0.3001
0.03	3.1952	1.5990	0.5619	1.3051	1.4752	1.6567	1.8434	0.3048
0.1	2.7980	1.3522	0.7423	1.5427	1.7163	1.8650	1.9665	0.3680
0.2	2.2520	1.1423	1.2094	1.6823	1.8011	1.8949	1.9614	0.6061
0.3	1.8694	1.0681	1.5914	1.6100	1.7330	1.8399	1.9292	0.7840
0.4	1.6132	1.0360	1.7980	1.5399	1.6743	1.7966	1.9056	0.8836
0.5	1.4337	1.0195	1.9005	1.4929	1.6357	1.7686	1.8904	0.9406
0.7	1.2003	1.0049	1.9784	1.4455	1.5968	1.7406	1.8753	0.9945
1.0	1.0000	1.0000	2.0000	1.4286	1.5830	1.7306	1.8700	1.1032

TABLE 1. Values of R_c, α_c, Nu_2, $c_4(\frac{1}{2}\pi)$, $c_4(\frac{1}{3}\pi)$, $c_4(\frac{1}{4}\pi)$, $c_4(\frac{1}{6}\pi)$ and c_2 for different permeability ratios for the closed-top Donaldson (1962) problem

K_1/K_2	R_c	α_c/π	Nu_2	$c_4(\frac{1}{2}\pi)$	$c_4(\frac{1}{3}\pi)$	$c_4(\frac{1}{4}\pi)$	$c_4(\frac{1}{6}\pi)$	$10c_2$
0.00001	2.2151	1.2438	0.4442	1.7462	1.8024	1.8625	1.9279	0.5273
0.00003	2.2150	1.2438	0.4442	1.7462	1.8024	1.8626	1.9279	0.5280
0.0001	2.2147	1.2436	0.4442	1.7464	1.8026	1.8627	1.9280	0.5274
0.0003	2.2139	1.2431	0.4443	1.7470	1.8031	1.8632	1.9283	0.5276
0.001	2.2112	1.2415	0.4447	1.7489	1.8049	1.8648	1.9294	0.5287
0.003	2.2033	1.2369	0.4458	1.7545	1.8101	1.8692	1.9324	0.5313
0.01	2.1755	1.2208	0.4500	1.7740	1.8282	1.8845	1.9426	0.5408
0.03	2.0954	1.1755	0.4648	1.8290	1.8774	1.9245	1.9674	0.5723
0.06	1.9749	1.1119	0.4968	1.9013	1.9382	1.9697	1.9921	0.6326
0.1	1.8195	1.0405	0.5597	1.9652	1.9870	2.0017	2.0068	0.7336
0.2	1.4936	0.9283	0.7953	2.0025	2.0096	2.0119	2.0088	0.9938
0.3	1.2635	0.8702	1.0591	1.9852	1.9943	2.0000	2.0020	1.1808
0.4	1.1017	0.8347	1.2895	1.9582	1.9730	1.9851	1.9942	1.3028
0.5	0.9840	0.8097	1.4738	1.9304	1.9515	1.9703	1.9865	1.3850
1.0	0.6864	0.7405	1.9537	1.8326	1.8768	1.9196	1.9607	1.5584

TABLE 2. Values of R_c, α_c, Nu_2, $c_4(\frac{1}{2}\pi)$, $c_4(\frac{1}{3}\pi)$, $c_4(\frac{1}{4}\pi)$, $c_4(\frac{1}{6}\pi)$, and c_2 for different permeability ratios for the open-top Donaldson (1962) problem

stable planform for convection, at least when the Rayleigh number is close to its critical value.

The second study is by Rana *et al.* (1979) who considered large-amplitude convection in a model of the Pahoa reservoir in Hawaii. They considered three cases of this open-top three-layer system, the first two had heated vertical boundaries and therefore we cannot apply our method. The third case had insulated sidewalls which, for porous media convection, is equivalent to fixing the wavenumber in an infinite layer since slip boundary conditions apply. The parameters they quote have been presented in the appropriate form for this study by McKibbin & O'Sullivan (1981) and are $r_1 = 0.4375$, $r_2 = 0.25$, $r_3 = 0.3125$, $K_2/K_1 = 0.4$, $K_3/K_1 = 2.5$ and $k_1 =$

ϕ	$c_4(\phi)$	ϕ	$c_4(\phi)$
0°	2.00000	50°	2.01773
10°	2.00097	60°	2.02220
20°	2.00373	70°	2.02569
30°	2.00786	80°	2.02789
40°	2.01275	90°	2.02864

TABLE 3. Values of $c_4(\phi)$ for the Rana *et al.* (1979) problem

$k_2 = k_3$. The lowest sublayer (sublayer 1) is taken as the reference. Rana *et al.* considered a two-dimensional cavity of aspect ratio 2 (width/height) and calculated the critical Rayleigh number to be $R_c = 0.83834$ and the corresponding wavenumber, $\alpha_c = \pi$. In a layer of infinite horizontal extent the critical Rayleigh number is reduced to 0.77155 at a wavenumber of 0.72351π. Values of Nu_2 and c_2 for this case are 1.52198 and 0.15907, respectively. In table 3 we present values of c_4 as a function of ϕ for the infinite layer. We note that $c_4(\phi) \geqslant 2$ for all ϕ and it varies by less than 1.5%. Thus the sideband instability is the predominant instability mechanism for positive K and rolls again constitute the stable planform.

8. Discussion

We have considered the onset and three-dimensional stability of convection in a fluid-saturated porous layer, heated from below and consisting of homogeneous horizontal sublayers. In particular, we have analysed configurations consisting of two sublayers and symmetric layers comprising three sublayers. The marginal curves for the onset of convection have been calculated and we have presented contour plots of the critical Rayleigh numbers. Prominent features of these plots are the loci of double-minimum points where two modes of differing wavenumbers onset simultaneously. These are significant, for rich dynamical behaviour has been found in such situations where the wavenumbers are commensurate: interesting phenomena such as travelling waves and homoclinic orbits occur.

A weakly nonlinear analysis was presented for the general case of one global minimum in the neutral curve; we hope to pursue the special case of two minima in future work. Utilizing a pressure–temperature formulation of the governing equations, we were able to investigate the three-dimensional stability properties of the finite-amplitude convection. In direct contrast to McKibbin & O'Sullivan (1981), we find that the governing (linearized) system may be made self-adjoint (but only if the thermal properties of the sublayers are identical) by a suitable weighting of the equations in each sublayer. Thus whereas McKibbin & O'Sullivan resorted to a direct numerical solution of the third-order equations to determine the solvability condition, we find a simple analytic form. This enabled Landau–Ginzburg equations governing the amplitudes of various two-dimensional modes to be derived more easily.

As in Rayleigh–Bénard convection, the sideband-instability curve ($\sigma = 3c_2K^2$) may be deduced directly from the curvature of the neutral curve at its base, and the zigzag instability is active when the wavenumber of the fluid motion is less than the critical wavenumber. We have determined (i) the relative importance of the cross-roll and sideband instabilities for rolls, (ii) the stability of rolls and square cells and (iii)

the relative importance of the sideband and an oblique mode instability for square cells.

For two-layer configurations the sideband instability turns out to be a more important instability mechanism than the cross-roll one over much of parameter space, although the cross-roll instability is more important for a single layer. We find that there is a locus of double-minimum points along which two modes of differing wavenumbers have simultaneous onset and the end of which corresponds to a quartic turning point in the neutral curve. A singularity lying on the locus was revealed and traced to the presence of resonant forcing terms at second order; in this case the solvability condition at second order yields sets of quadratic-amplitude equations. This resonance phenomenon occurs at all points on the double-minimum locus. Thus there must exist a region, not necessarily small, surrounding the double-minimum locus where the present analysis does not apply; the extent of such a region is unknown owing to the local nature of weakly nonlinear analysis and can only be deduced by using a suitable fully nonlinear numerical method.

For symmetric three-layer configurations there are two double-minimum loci, one of which occurs when the middle sublayer is more permeable than the outer layers, the other when it is less permeable. When the middle layer is more permeable the cross-roll instability is the dominant instability mechanism. The corresponding double-minimum locus is found to occur entirely within a region where the cross-roll instability mechanism is sufficiently strong as to render rolls unstable and square cells stable. When the middle sublayer is less permeable, the sideband instability becomes the more important instability over much of parameter space.

On the double-minimum loci no second-order resonances arise, as shown by symmetry arguments, but third-order resonances may occur. Although they are not analysed here there is, in fact, a considerable number of these resonances but their influence is felt only within an $O(\epsilon^2)$-distance of the double-minimum locus.

Although we have restricted ourselves by assuming identical thermal properties in each sublayer and considering only two specific configurations, we may, nevertheless, make some informed comments about other configurations based on the qualitative features of the present results and the role played by symmetry. The presence of a double-minimum locus seems to be a general feature, and it is possible to find certain configurations for which there are three minima (see figure 12). If the parameter values are close to those on a double-minimum locus, the effects of resonance between the modes of different wavenumbers will depend on the symmetry of the layer in the way that we have found here. Open-top layers cannot be considered as symmetric, but it may be possible to approach symmetry fairly closely either by having almost impermeable upper and lower sublayers, or by having a very thin, but highly permeable, lower sublayer. Of course, the symmetric layer cannot be regarded as typical for a perturbation in its parameters will contain an antisymmetric component, in general. Indeed it may be shown that an $O(\epsilon)$ antisymmetric perturbation will generate quadratic terms in the third-order amplitude equations when the parameters lie within $O(\epsilon^2)$ of the double-minimum locus. In this way it would be possible to have some idea of the expected phenomena near the double-minimum locus for general asymmetric layers. We hope to return to this at a later date.

The effect on finite-amplitude convection of different thermal properties in each layer is unknown. All that may be said with certainty is that double- (and multiple-) minimum loci do exist for this more general problem. Although we believe that the same qualitative results apply (such as the supercritical bifurcation of single-roll

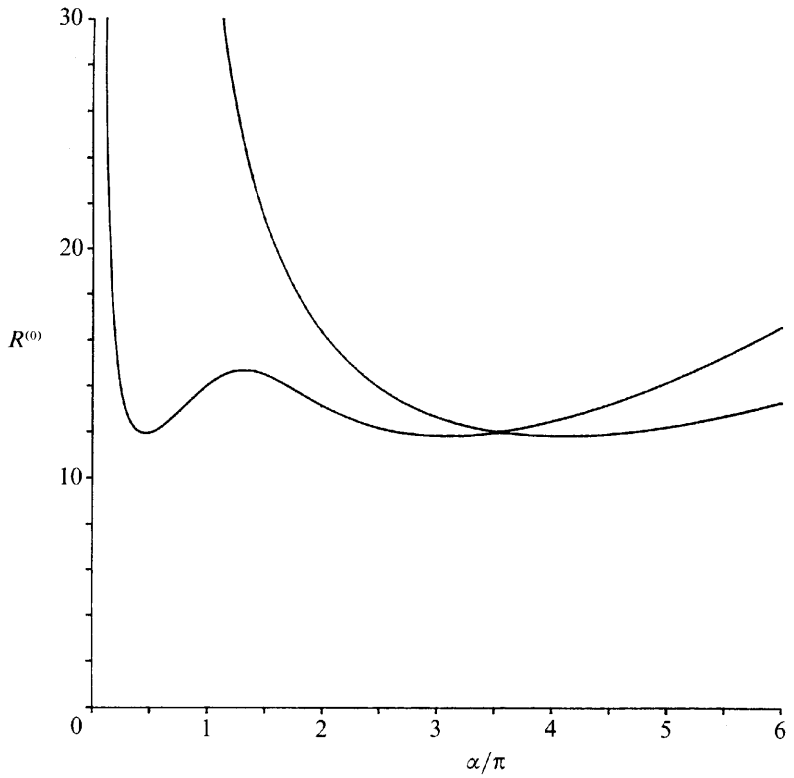

FIGURE 12. Marginal curves for the first two modes for a non-symmetric three-layer system displaying three minima simultaneously. The values of the defining parameters are: $r_1 = 0.26$, $r_2 = 0.539056$, $r_3 = 0.200944$, $K_2/K_1 = 0.0214724$, $K_3/K_1 = 1.7$ and $k_1 = k_2 = k_3$. The critical Rayleigh number is 11.932788 and the critical wavenumbers are 0.455707π, 3.076458π and 4.081870π. For this general three-layer system there still remain two free parameters (say K_3/K_1 and r_1) which may be varied to track loci of triple-minimum points.

modes, and the absence of resonant-forcing terms at second order) we cannot easily prove it since we lack an analytic form for the solvability condition.

Recent work by Rees & Riley (1986, 1987, 1989*a*, *b*) and Rees (1990) on the effect on convection in a single layer of non-uniform boundary conditions such as undulating isothermal boundaries or non-uniformly heated plane boundaries, has shown that there exists a vast array of different types of cellular planform which are linearly stable. The presence of thermal non-uniformities and undulations is well known in the geothermal context and it is natural to question the combined effects of both non-uniformities and layering. This is a project of considerable algebraic complexity, but it is possible to infer some of the qualitative features of the resulting flows. Assuming that the parameters are far from a double-minimum locus and that the stable mode in the absence of imperfections is the roll, then the results summarized above should apply for the composite problem also. If square cells were stable for the unmodulated problem, it would then be possible to use the amplitude equations derived in Rees & Riley (1989*a*) for this imperfection.

D. A. S. R. would like to acknowledge SERC support during the preparation of this work; D. S. R. wishes to thank Stephen Davis for his hospitality at Northwestern University during the final preparation of the paper. The authors would like to thank the referees for constructive criticism on the presentation of the paper.

REFERENCES

ARMBRUSTER, D., GUCKENHEIMER, J. & HOLMES, P. 1988 Heteroclinic cycles and modulated travelling waves in systems with $O(2)$ symmetry. *Physica* **29D**, 257–282.

BECK, J. L. 1972 Convection in a box of porous material saturated with fluid. *Phys. Fluids* **15**, 1377–1383.

CALTAGIRONE, J. P. 1975 Thermoconvective instabilities in a horizontal porous layer. *J. Fluid Mech.* **72**, 269–287.

CATTON, I. & LIENHARD, J. H. 1984 Thermal stability of two fluid layers separated by a solid interlayer of finite thickness and thermal conductivity. *Trans. ASME* C: *J. Heat Transfer* **106**, 605–612.

CHEN, F. & CHEN, C. F. 1988 Onset of finger convection in a horizontal porous layer underlying a fluid layer. *Trans. ASME* C: *J. Heat Transfer* **110**, 403–409.

DONALDSON, I. G. 1962 Temperature gradients in the upper layers of the earth's crust due to convective water flows. *J. Geophys. Res.* **67**, 3449–3459.

GEORGHITZA, ST. I. 1961 The marginal stability in porous inhomogeneous media. *Proc. Camb. Phil. Soc.* **57**, 871–877.

GEORGIADIS, J. G. & CATTON, I. 1986 Prandtl number effect on Bénard convection in porous media. *Trans. ASME* C: *J. Heat Transfer* **108**, 284–289.

HEIBER, C. A. 1987 Multilayer Rayleigh–Bénard instability via shooting method. *Trans. ASME* C: *J. Heat Transfer* **109**, 538–540.

HORTON, C. W. & ROGERS, F. T. 1945 Convection currents in a porous medium. *J. Appl. Phys.* **16**, 367–370.

IMPEY, M. D., RILEY, D. S. & WINTERS, K. H. 1990 The effect of sidewall imperfections on pattern formation in Lapwood convection. *Nonlinearity* **3**, 1–14.

JONES, C. A. & PROCTOR, M. R. E. 1988 Strong spatial resonance and travelling waves in Bénard convection. *Phys. Lett.* A **121**, 224–228.

KATTO, Y. & MASUOKA, T. 1967 Criterion for the onset of convective flow in a fluid in a porous medium. *Intl J. Heat Mass Transfer* **10**, 297–309.

KVERNVOLD, O. & TYVAND, P. A. 1979 Nonlinear thermal convection in anisotropic porous media. *J. Fluid Mech.* **90**, 609–624.

KVERNVOLD, O. & TYVAND, P. A. 1980 Dispersion effects on thermal convection in porous media. *J. Fluid Mech.* **99**, 673–686.

LAPWOOD, E. R. 1948 Convection of a fluid in a porous medium. *Proc. Camb. Phil. Soc.* **44**, 508–521.

LIENHARD, J. H. & CATTON, I. 1986 Heat transfer across a two-fluid layer region. *Trans. ASME* C: *J. Heat Transfer* **108**, 198–205.

MCKIBBIN, R. 1983 Convection in an aquifer above a layer of heated impermeable bedrock. *New Zealand J. Sci.* **26**, 49–64.

MCKIBBIN, R. & O'SULLIVAN, M. J. 1980 Onset of convection in a layered porous medium heated from below. *J. Fluid Mech.* **96**, 375–393.

MCKIBBIN, R. & O'SULLIVAN, M. J. 1981 Heat transfer in a layered porous medium heated from below. *J. Fluid Mech.* **111**, 141–173.

MCKIBBIN, R. & TYVAND, P. A. 1983 Thermal convection in a porous medium composed of alternating thick and thin layers. *Intl J. Heat Mass Transfer* **26**, 761–780.

MCKIBBIN, R. & TYVAND, P. A. 1984 Thermal convection in a porous medium with horizontal cracks. *Intl J. Heat Mass Transfer* **27**, 1007–1023.

MASUOKA, T., KATSUHARA, T., NAKAZONO, Y. & ISOZAKI, S. 1979 Onset of convection and flow patterns in a porous layer of two different media. *Heat Transfer: Japan. Res.* **7**, 39–52.

NEWELL, A. C. & WHITEHEAD, J. A. 1969 Finite bandwidth, finite amplitude convection. *J. Fluid Mech.* **38**, 279–303.

PALM, E., WEBER, J. E. & KVERNVOLD, O. 1972 On steady convection in a porous medium. *J. Fluid Mech.* **54**, 153–161.

PILLATSIS, G., TASLIM, M. E. & NARUSAWA, U. 1987 Thermal instability of a fluid-saturated porous medium bounded by thin fluid layers. *Trans. ASME* C: *J. Heat Transfer* **109**, 677–682.

PROCTOR, M. R. E. & JONES, C. A. 1988 The interaction of two spatially resonant patterns in thermal convection. Part 1. Exact 1:2 resonance. *J. Fluid Mech.* **188**, 301–335.

RANA, R., HORNE, R. N. & CHENG, P. 1979 Natural convection in a multi-layered geothermal reservoir. *Trans. ASME* C: *J. Heat Transfer* **101**, 411–416.

REES, D. A. S. 1990 The effects of long wavelength boundary imperfections on the onset of convection in a porous layer. *Q. J. Mech. Appl. Maths* (to appear).

REES, D. A. S. & RILEY, D. S. 1986 Free convection in an undulating saturated porous layer: resonant wavelength excitation. *J. Fluid Mech.* **166**, 503–530.

REES, D. A. S. & RILEY, D. S. 1987 The evolution of instabilities in an infinite porous layer heated from below: the effect of near-resonant thermal forcing. In *Bifurcation Phenomena in Thermal Processes and Convection, ASME Winter Annual Meeting, Boston, 1987. ASME HTD* vol. 94, *AMD* vol. 89, pp. 59–66.

REES, D. A. S. & RILEY, D. S. 1989*a* The effects of boundary imperfections on convection in a saturated porous layer: near-resonant wavelength excitation. *J. Fluid Mech.* **199**, 133–154.

REES, D. A. S. & RILEY, D. S. 1989*b* The effects of boundary imperfections on convection in a saturated porous layer: non-resonant wavelength excitation. *Proc. R. Soc. Lond.* A **421**, 303–329.

RIAHI, N. 1983 Nonlinear convection in a porous layer with finite conducting boundaries. *J. Fluid Mech.* **129**, 153–171.

RIBANDO, R. & TORRANCE, K. E. 1976 Natural convection in a porous medium: effects of confinement, variable permeability, and thermal boundary conditions. *Trans. ASME* C: *J. Heat Transfer* **98**, 42–48.

RILEY, D. S. & DAVIS, S. H. 1989 Eckhaus instabilities in generalized Landau–Ginzburg equations. *Phys. Fluids* A **1**, 1745–1747.

RILEY, D. S. & WINTERS, K. H. 1989*a* Modal exchange mechanisms in Lapwood convection. *J. Fluid Mech.* **204**, 325–358.

RILEY, D. S. & WINTERS, K. H. 1989*b* Time-periodic convection in porous media: the evolution of Hopf bifurcations with aspect ratio. In preparation.

SCHLÜTER, A., LORTZ, D. & BUSSE, F. H. 1965 On the stability of steady finite-amplitude convection. *J. Fluid Mech.* **23**, 129–144.

SOMMERTON, C. W. & CATTON, I. 1982 On the thermal instability of superposed porous and fluid layers. *Trans. ASME* C: *J. Heat Transfer* **104**, 160–165.

STRAUS, J. M. 1974 Large amplitude convection in porous media. *J. Fluid Mech.* **64**, 51–63.

STRAUS, J. M. & SCHUBERT, G. 1981 Modes of finite-amplitude three-dimensional convection in rectangular boxes of fluid-saturated porous material. *J. Fluid Mech.* **103**, 23–32.

WESTBROOK, D. R. 1969 Stability of convective flow in a porous medium. *Phys. Fluids* **12**, 1547–1551.